# Programmed inhibition of an innate immune receptor via *de novo* designed transmembrane proteins

**Maillie, C.A., Zhang, M. Goiset, M., Goldenfeld, G., Ward, A.B.*, Mravic, M.***

[1]Department of Integrative Structural and Computational Biology, The Scripps Research Institute, La Jolla, CA, 92037, USA

*Corresponding authors:
Marco Mravic, mmravic@scripps.edu
Andrew Ward, andrew@scripps.edu

**Attributions of credit:**
CAM (Conceptualization, Data curation, Formal analysis, Writing – original draft, Writing – review and editing); MZ (Data curation); NG (Data curation); GG (Data curation); ABW (Resources, Conceptualization, Supervision, Writing – review and editing); MM (Resources, Conceptualization, Data curation, Formal analysis, Supervision, Writing – review and editing)

## Abstract

Toll-like receptors (TLRs) are single-pass membrane proteins central to innate immunity, yet the role of homodimeric transmembrane (TM) domain interactions in cross-membrane signaling remains poorly understood and underexploited for therapeutic intervention. Here, we conduct a *de novo* computational design campaign to generate synthetic peptides that selectively target the TM domain of Toll-like receptor 4 (TLR4), a key mediator of inflammatory signaling and a clinically relevant drug target. Using in silico modeling and cell-based screening, we identified two peptides that disrupt membrane-embedded interactions essential for receptor activation. Our lead candidate binds sequence-specifically to the native TM-juxtamembrane region, acting as a largely target-selective and preliminarily dose-dependent inhibitor that impairs TLR4 signaling without affecting receptor expression. This work establishes a novel inhibitory mechanism based on structural perturbation of the TM interface and provides a generalizable framework for designing TM-targeting molecules in the absence of structural or evolutionary templates. These findings underscore the functional importance of membrane-spanning interactions and open a new therapeutic avenue for modulating TLR4 activity in the context of infection, autoimmunity, and inflammation.

## Introduction

Targeting native protein-protein interactions within the membrane-spanning regions of single-pass transmembrane receptors has emerged as a promising strategy for antagonizing diverse signaling pathways. This approach has demonstrated success across several receptor families, including receptor tyrosine kinases, integrins, and the T cell receptor (TCR)[1–6]. Notably, the TM domain of TLR2 has been shown to act as a blockade molecule that disrupts heterodimeric complexes involved in specific signaling events[7,8].

Although TM dimerization has been observed, a TM-targeting strategy remains underexplored across the broader TLR family[9]. Our recent findings support a biologically active role for the TM domain in the structure–function relationship of TLR4 signaling, suggesting a rigorous investigation into TM-mediated inhibition within the TLR family holds potential to not only advance mechanistic understanding[10,11]. Furthermore, various TLR4 inhibitors have failed in clinical trials, so TM targeted antagonists could also unlock novel opportunities for therapeutic intervention[12,13].

Both endogenous and synthetic TM peptides have proven effective in disrupting TM dimer complexes, each offering distinct advantages. Peptides derived from native TM sequences have been used to target full-length receptors, effectively shifting the equilibrium of signaling competent receptor complexes to inactive receptor populations[14–18]. These endogenous TM peptides exploit the inherent ability of specific TM domains to engage in homo- or hetero-dimerization. For receptors where such dimerization propensities are well-characterized and widely accepted as physiologically relevant, targeting with native sequences offers a rapid and accessible approach for developing functional inhibitors and testing mechanistic hypotheses using readily available peptide sequences.

In contrast, computational design presents an opportunity to optimize TM-targeting peptides for enhanced affinity, specificity, and favorable biophysical properties[19–21]. In silico methods can be used to simultaneously engineer functional probes and gain insight into the fundamental principles governing protein–protein interactions within the membrane. Successful TM-targeting molecules designed to date often exhibit key features such as interfacial hydrogen bonding and tightly packed apolar side chains[2–6,22,23]. However, previous computational design approaches have relied heavily on the availability of structural templates and known dimerization motifs, two elements that are currently unavailable for TLR4[3,4,24,25]. The lack of a common interaction motif and the limitations of current prediction methods to converge on a confident TM dimer model make TLR4 particularly resistant to traditional design strategies. As such, *de novo* design of TM-targeting molecules for TLR4 represents an unmet challenge. Addressing this challenge would not only enable the development of TLR4-specific inhibitors, but also establish a broader framework

for designing synthetic peptides against other transmembrane domains that lack canonical dimerization features.

In this study, we hypothesized that the largely apolar transmembrane domain of TLR4 inherently encodes molecular recognition and can be synthetically optimized to regulate signal transmission across the lipid bilayer. Using cell-based biochemical assays, we identified that TLR4 molecular interactions within the lipid bilayer are both physiologically relevant and necessary for receptor activation. We also developed a versatile and robust in silico protein design method to generate *de novo* membrane-targeting molecules. With this advancement, we isolated sequence-specific TLR4 TM adaptor molecules and proactively tested their ability to inhibit receptor activity Functional assays using both native and designed TM-targeting peptides demonstrate that disrupting this TM dimerization impairs receptor activation, highlighting its essential role. One successful design inhibited TLR4 function upon LPS challenge, forming stable interactions with the TLR4 TM domain both in cells and in vitro. Our lead molecule exhibited sequence-specific, dose-dependent behavior and demonstrated limited off-target interactions. This protein engineering campaign represents a significant advancement in membrane protein design and our understanding of TLR4 mechanisms. Our results provide insights into a more integrated cross-membrane signaling mechanism for full-length receptors and offer a framework for future therapeutic strategies that consider receptor TM dimerization in their mechanisms of action. Furthermore, we present a novel approach for computationally designing membrane protein adaptor molecules, greatly expanding the potential to target a diverse range of TM receptors.

## Results

### TLR4 and a TLR4 TM peptide self-associate in cells

We initially evaluated the capacity for the TLR4 TM domain to oligomerization in a cellular context by assessing homodimerization relevance in the lipid bilayer of mammalian cells. To quantify these interactions, we adapted a split-enzyme cell-based assay by fusing TLR4-eGFP or its TM sequence to either

the smallBit or largeBit component of NanoLuc (Fig. 4.1A,D)[26]. Proximity-induced enzyme complementation generates a luminescent signal upon substrate addition, serving as a direct readout of protein-protein interactions (PPIs). To normalize for expression levels, we then introduce a competitive HiBit peptide, which displaces smallBit binding and provides an internal reference. Widefield microscopy confirmed robust plasma membrane localization of TLR4-eGFP and TLR4 TM constructs in 293T cells (Figure 1B,E). Across three biological replicates, TLR4-eGFP and TM constructs exhibited significantly higher (>100 fold, $p < 0.005$) normalized luminescence than the negative control (eVgL, a non-interacting synthetic design). Both TLR4-eGFP and TM self-interactions also exceeded heterooligomer interactions with CD8α-TMJM, a promiscuous receptor used as a non-specific interaction control ($p < 0.005$ and $p < 0.05$, respectively) (Fig. 4.1C,F, Figure 2). These findings establish a physiologically relevant molecular interface within the membrane, independent of chemical agonists or antagonists, presenting a new opportunity for tuning TLR4 signaling mechanisms via the membrane spanning regions.

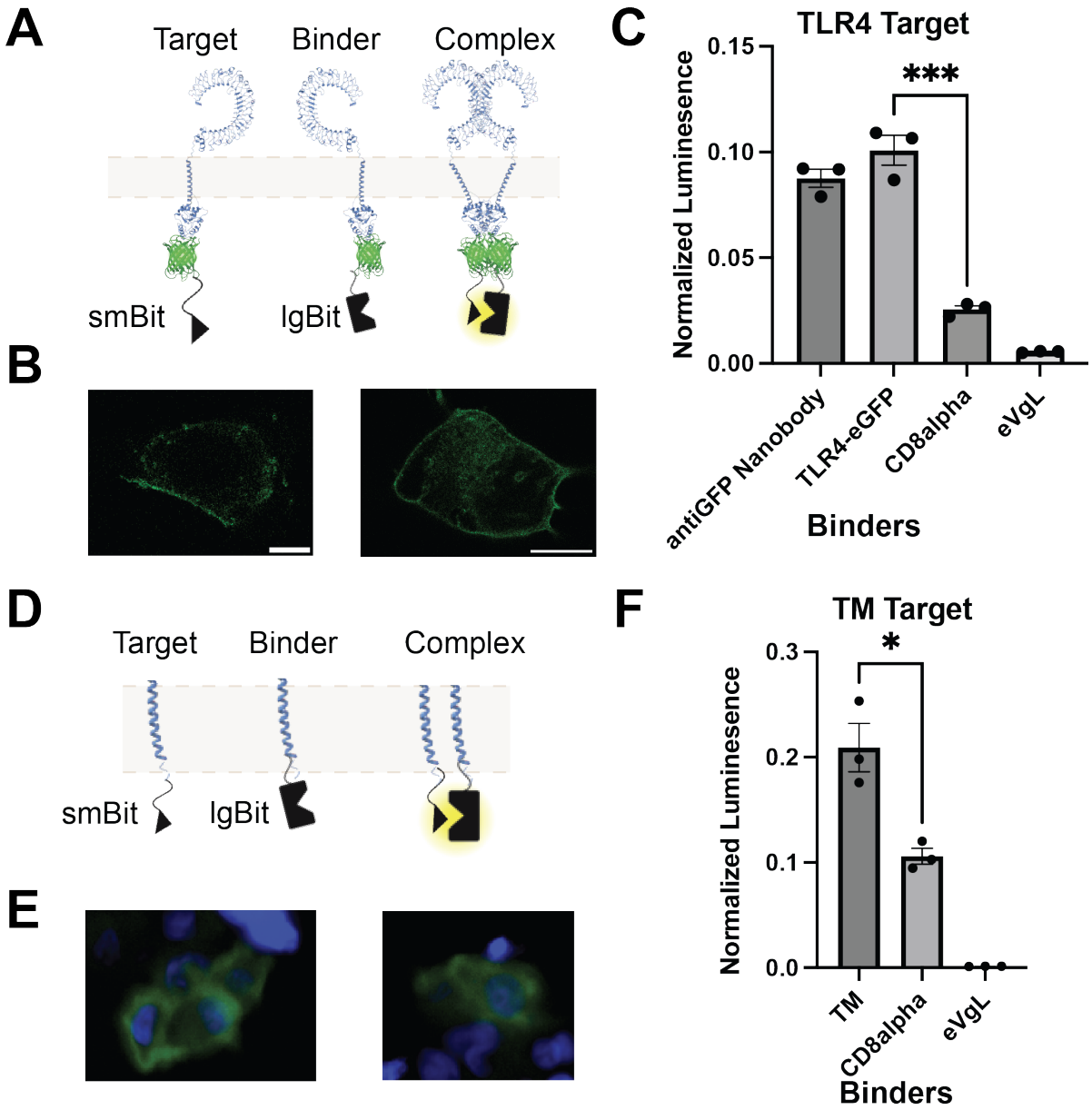


**Figure 1. TLR4 and isolated TM domains interact with themselves in mammalian cell membranes.** **A)** Target and binder constructs used to measure TLR4 protein-protein interactions in the NanoBit assay include a full-length receptor fused to eGFP and a smBit or lgBit component of the enzyme. A TLR4 homodimer complex will induce self-complementation of the NanoBit enzyme parts and produce luminescence upon addition of substrate. **B)** Confocal microscopy of U20S cells transfected with TLR4-eGFP target or binder constructs display trafficking to plasma membrane. Scale bars are 10um. **C)** Normalized luminescence for TLR4-eGFP target show significant self-interaction with corresponding binder constructs compared to non-specific (CD8alpha) and negative control (eVgL) binders (representative of n=3, biological replicates in Figure 2). **D)** Target and binder constructs used to measure isolated TM domain protein-protein interactions in the NanoBit assay. **E)** Widefield microscopy of 293T. cells transfected with TM fragment target or binder constructs display efficient expression and localize predominantly to plasma membrane. **F)** Normalized luminescence for TLR4 (left) or isolated TM (right) targets show significant self-interaction with corresponding TM binder construct compared to non-specific (CD8alpha) and negative control (eVgL) binders (representative of n=3, biological replicates in Figure 2).

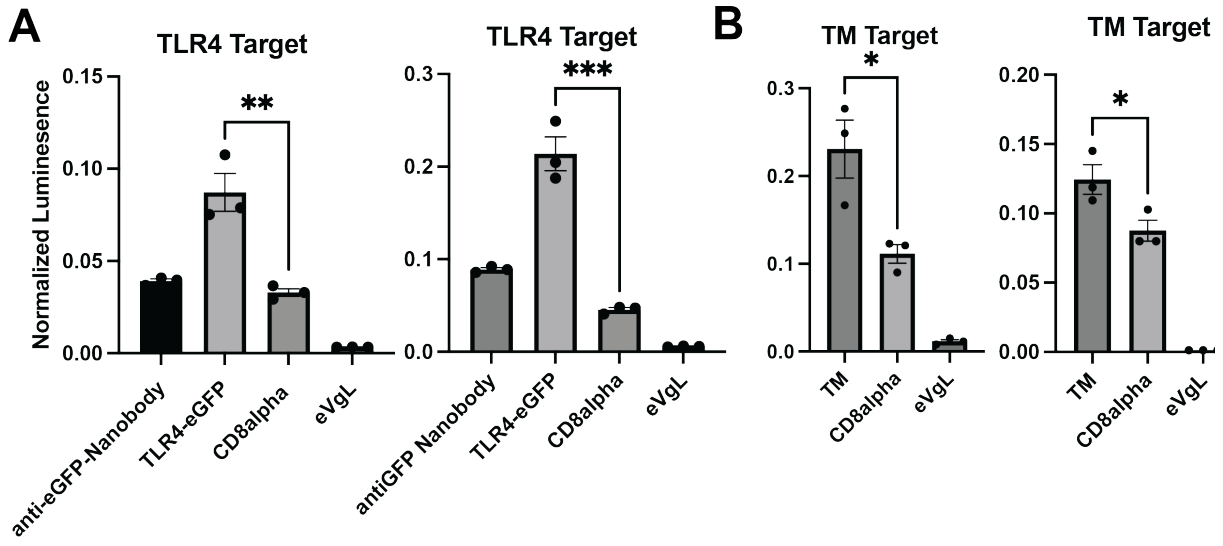


**Figure 2 NanoBit assay quantifies protein-protein interactions in cell membranes. A)** Biological replicates of NanoBit luminescence (smBit-LgBit interaction) normalized to HiBit luminescence (lgBit expression) establish TLR4-eGFP target and binder interacts with itself significantly more so than CD8alpha and eVgL. **B)** Corresponding analysis of biological replicates for minimal TLR4-TM domain target and binder constructs.

## Computational design of *de novo* TM peptides targeting the TLR4 TM domain

We then reasoned that the TLR4 TM helix presents malleable surfaces for engineering synthetic protein-protein interactions. Targeting TLR4 in this manner also requires tackling an underlying fundamental challenge in membrane protein design: can protein-protein interactions within the membrane be encoded for binding primarily apolar single-span TM domains in a sequence-specific manner, particularly that TLR4's dimerization interface is unknown and lacks an apparent motif sequence.

Previous computational efforts to design TM adaptors have relied on canonical interaction motifs (G-$X_3$-G, small-$X_3$-small), experimentally derived structural templates, or endogenously interacting sequences as starting scaffolds. Here, we expand and implement a ***de novo*** computational design method to develop synthetic TM peptides that target TLR4 independently of the structural or sequence context of the native interface. To guide design, we predicted homodimeric TLR4 TM complexes using AlphaFold2 multimer, an evolutionary based deep learning model for structural prediction, and TMHop, a Rosetta physics-based fold-and-dock algorithm including a lipophilicity term for predicted transmembrane helix-

helix interactions[25,27]. We selected three hypothetical models and rationalized their use as practical starting structures based on of their high interfacial interface surface area, potential for high contact density knobs-in-holes packing or stabilizing polar interactions, and principally that their different geometries enabled design models to cover distinct helix surfaces of TLR4's TM span (Figure 3A). Using the Rosetta membrane framework, we fixed one chain of the backbone model with the native TLR4 TM sequence and designed the other chain as the synthetic adaptor peptide using a set of membrane-compatible amino acids[24]. Over three design rounds, generating 800 models per round, we eliminated amino acid choices at specific positions which consistently led to steric clashes or unfavorable rotamers. Designs were first filtered using a combinatorial threshold of a packing score and predicted interface energies. We then selected designs maximizing the favorable features of hydrogen bonds between chains and the number of tight knobs into hole sidechain packing interactions (Figure 3B). After selecting the set of *de novo* sequences, the final design step diversified the amino acids on the lipid-facing surface of each design to reflect the natural distribution of amino acids and remove potential self-interaction sequence patterns (Table 4.1). Interestingly, AlphaFold3 failed to accurately re-predict our design models (Figure 4).

| | |
|---|---|
| Design 1 | EAPLIVWLLLLITIFLLGICAFIIYLIKKLA |
| Design 2 | EAPLIVWLLLLITIFLLGIMAFIIYLMKKLA |
| Design 3 | EEPLIVLALIGIISLLIFIMFGIIWLMKK |
| Design 4 | EAPELWLILGLILAMILILTLLIATMKKLLG |
| Design 5 | EAPLLCWLNILITIFLIATLLLIMLKR |
| Design 6 | EAPLILWLLLGITAFLILLLIGICLLIMKKL |
| Design 7 | EAPLINWLIILITIFIIGTLILIIKK |
| Design 8 | EEPEVTLWITALCIMAILLITGVLFYLMKKD |
| Design 9 | EAPLIMWLAILITIFIIGLLIFIMLALLKKL |
| TLR4 TM | MNKTIIGVSVLSVLVVSVVAVLVYKF |

**Table 4.1 *De novo* designed transmembrane protein sequences**

We then opted to use molecular dynamics simulations of 500 ns in model POPC membranes as an additional validation stage, wherein we determined 9 designs that form stable complexes with a TLR4 TM domain *in silico* that motivated biochemical characterization in cells (Figure 3C). Altogether, this computational pipeline enables the rapid and accurate design of transmembrane interactors, robustly generating realistic TM-TM models that are stable in silico.

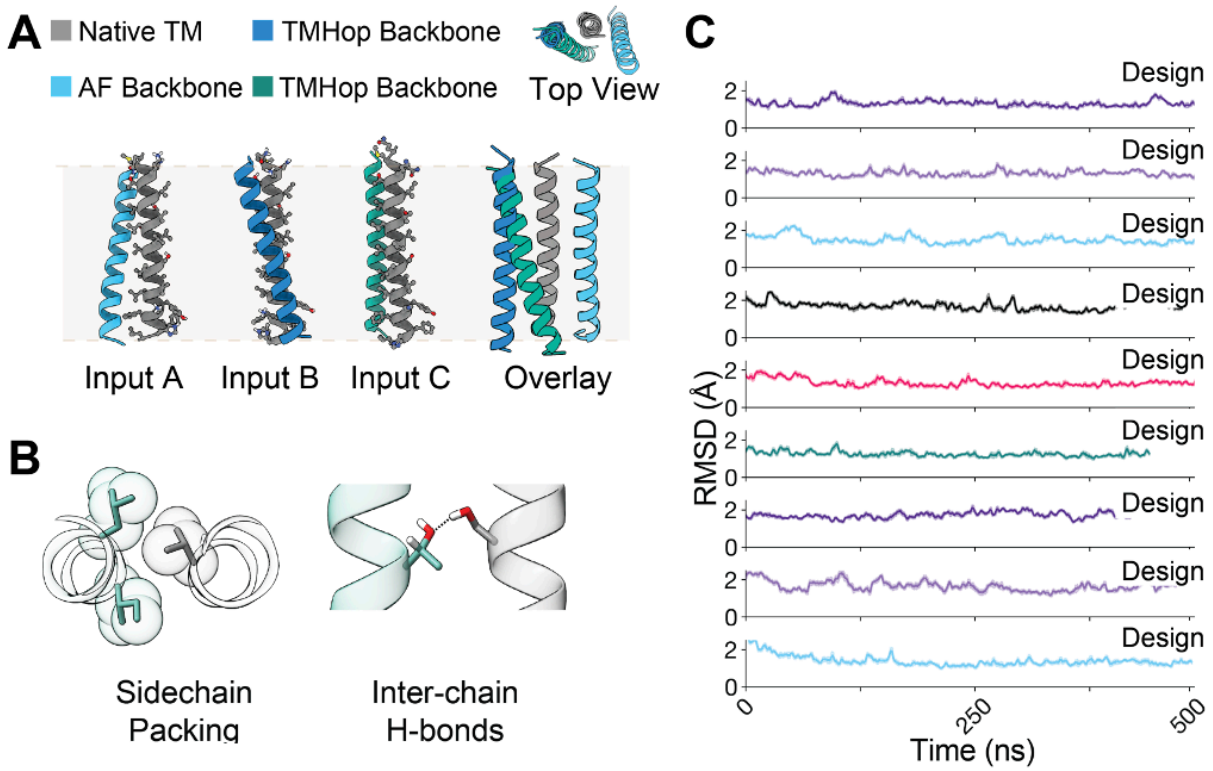


**Figure 3. Computational design of TLR4 targeting *de novo* transmembrane proteins**
**A)** Starting backbone models for anti-TLR4 TM targeting design were generated with AlphaFold2 or TMHop by predicting a TLR4 TM homodimer. Models with substantial interface area and covering diverse surfaces on the TLR4 TM helix were selected for design where one chain was fixed with the native TM sequence and the was variable in the subsequent sequence design process. **B)** *De novo* designs were filtered based on lowest predicted interface energies, maximum side chain packing, and optimized inter-chain hydrogen bonds. **C)** A set of 9 *de novo* designs were stable (mean backbone RMSD <2 Å ) throughout 500 ns MD simulations in model membranes and selected for further characterization.

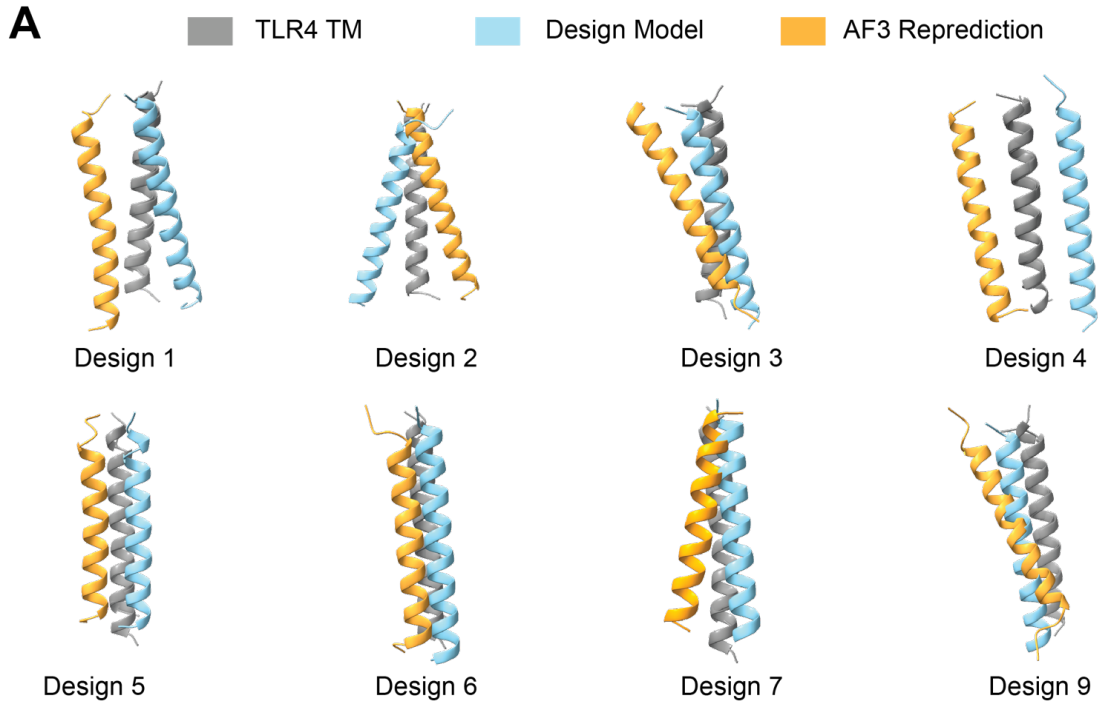


**Figure 4 Modern structural predictions do not accurately predict TM-Design interactions.**
TM interface interactions, helix geometry, and/or TM orientation from AlphaFold3 predictions of native TLR4 TM and *de novo* designs do not correspond to the design models.

## Sequence and target specific interactions between designs and TLR4 TMJM in cells.

To assess whether *de novo* peptides target the TLR4 TM domain and co-localize in mammalian cell membranes, we again adapted the NanoBit split-enzyme assay to evaluate protein-protein interactions (Figure 5A). We selected the minimal TLR4 TMJM fragment as the smallBit-tagged "Target" due to its favorable expression and performance in this assay. When tested against itself, the TMJM construct (SmBit-tagged "Target" co-expressed with largeBit-tagged "Binder") exhibited a >100-fold increase in split-enzyme complementation compared to the non-interacting negative control (eVgL LargeBit-tagged TM protein, Figure 6A), establishing a clear benchmark for positive interactions. Additionally, the normalized luminescence for self-interacting TMJM constructs was **2.2 ± 0.3-fold** higher than that of TMJM paired with a non-specific control (CD8α, a promiscuous receptor). In comparison, self-interactions of TLR4-eGFP-SmBit and TM-SmBit were only on average **2.0 ± 0.5-fold** and **1.8 ± 0.3-fold** higher than their interactions with CD8α-LargeBit, respectively. These results indicate that TMJM provides the more robust

and optimal dynamic range for assessing the interaction potential of designed constructs compared to full-length TLR4-eGFP or minimal TM as the "Target".

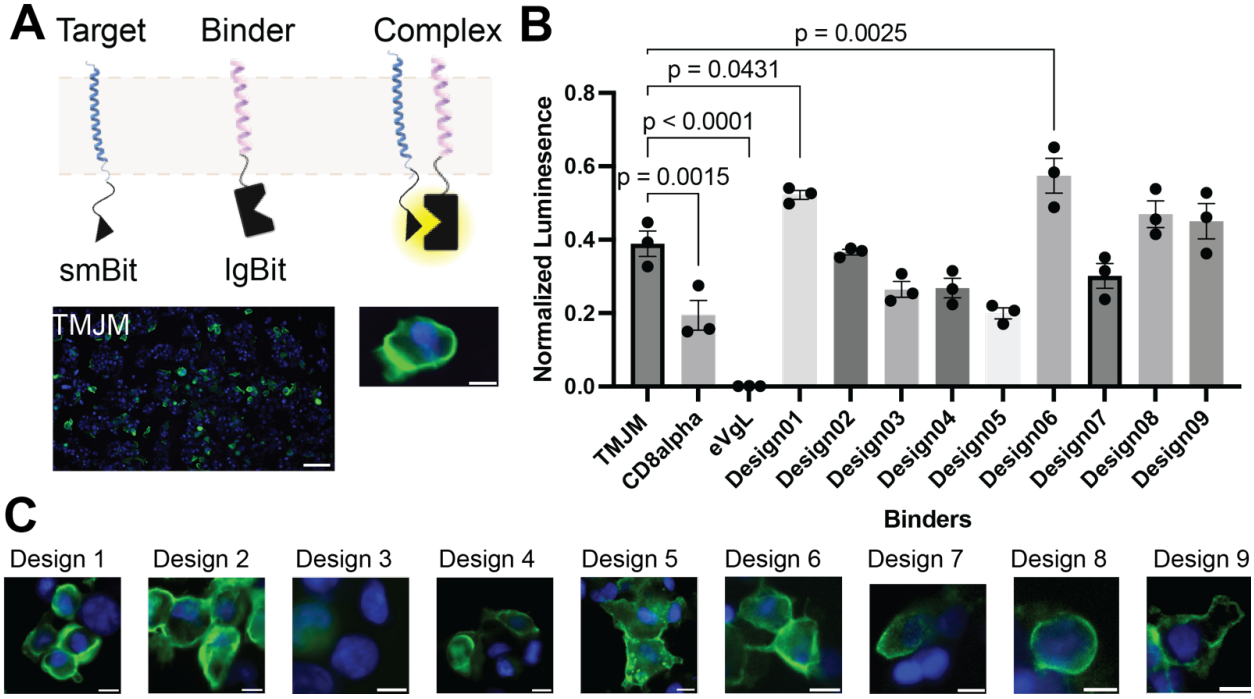


**Figure 5. Sequence-specific protein-protein interactions in cell membranes between *de novo* designs and the TLR4 TM domain**

**A)** TMJM fused to smBit component of NanoLuc enzyme was used as the target with *de novo* designed TM proteins fused to the lgBit component of NanoLuc to evaluate the interaction capacity with NanoBit in mammalian cell membranes. Expression and trafficking to plasma membrane was confirmed with Flag-immunostaining and widefield microscopy in 293T cells. **B)** NanoBit luminescence was normalized by HiBit luminescence to quantify protein-protein interaction in cell membranes and revealed that all 9 *de novo* designs formed significantly ($p<0.05$) more interaction with TMJM target than the non-specific control CD8alpha. Designs 1 and 6 had significantly ($p<0.05$) higher luminescence than the TMJM self-interacting positive control, qualifying these proteins as lead candidates. **C)** Majority of *de novo* designs expressed and trafficked to plasma membrane in a predominantly type I orientation when analyzed with Flag-immunostaining and widefield microscopy in 293T cells. Scale bar is 10 $\mu m$.

Following transient co-transfection of each designed TM protein with the TLR4 TMJM construct in HEK293T cells, widefield fluorescence microscopy confirmed robust expression and plasma membrane localization of the *de novo* designs (Figure 5C, Figure 6B). Since we performed Flag-tag immunostaining without membrane permeabilization, we conclude that the constructs predominantly insert in a type I orientation, supporting their potential to interact with TLR4 as designed and in a physiologically relevant manner. When tested against the TMJM target, all nine designs exhibited higher normalized luminescence than CD8α (Figure 5B, Figure 6C). Notably, Design 1 and Design 6 demonstrated exceptionally high

interaction potential, with an average **65±10%** and **99 ± 22% (n=3)** increases in normalized luminescence compared to the positive control, self-interacting TMJM. These results identify Designs 1 and 6 as lead anti-TLR4 TM protein candidates.

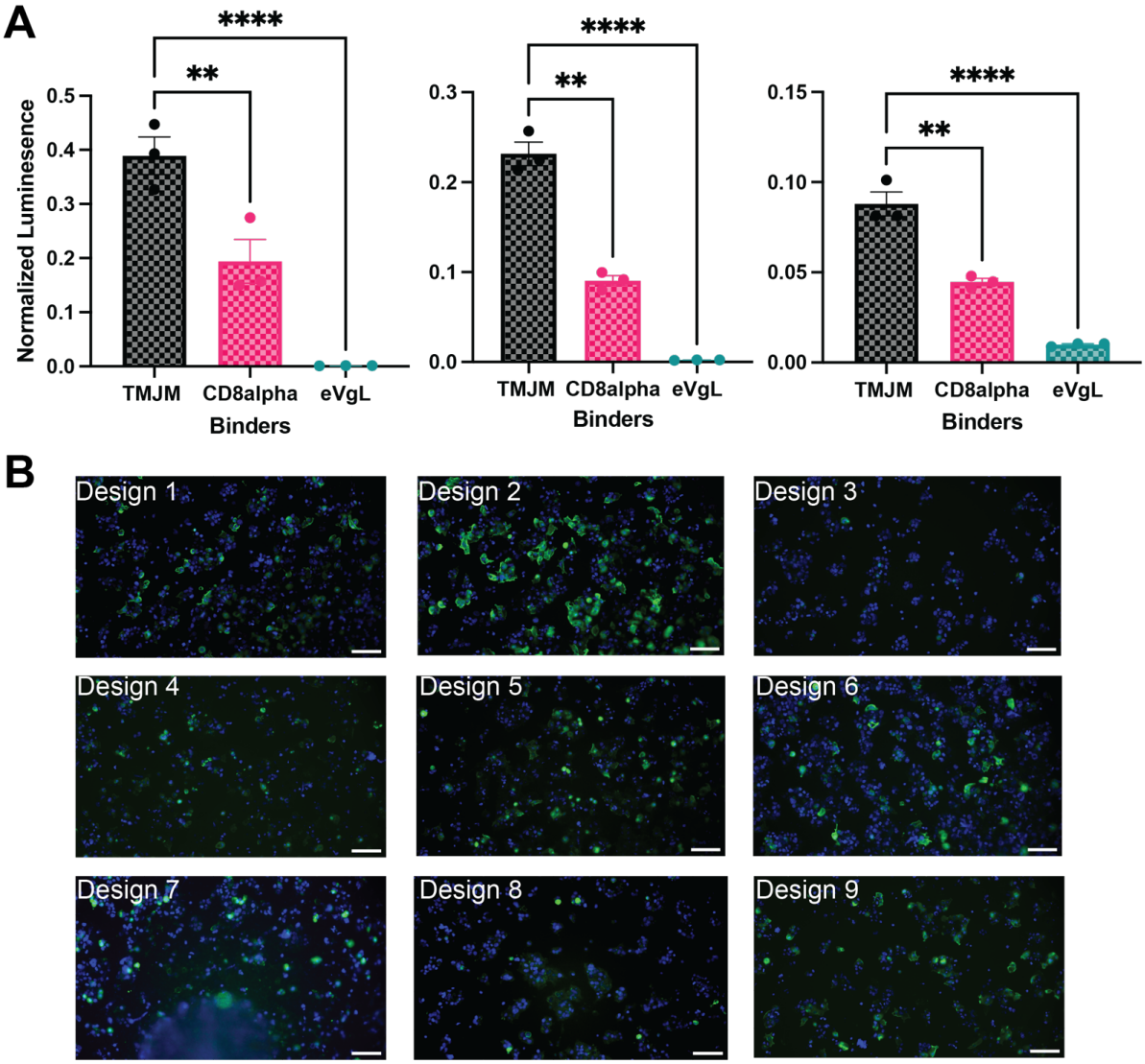


**Figure 6. TMJM target and *de novo* design binders for NanoBit assay. A)** A TMJM target is optimal for NanoBit assay to test *de novo* design interactions with a approximate 2 fold-change in normalized luminescence between non-specific control CD8alpha and >100 fold-change in normalized luminescence different between negative control eVgL. **B)** Immunostaining of *de novo* design expression constructs expressed 293T cells and with anti-Flag-Alexa488 staining shows all designs express and traffic to plasma membrane. Scale bar is 100 $\mu$m.

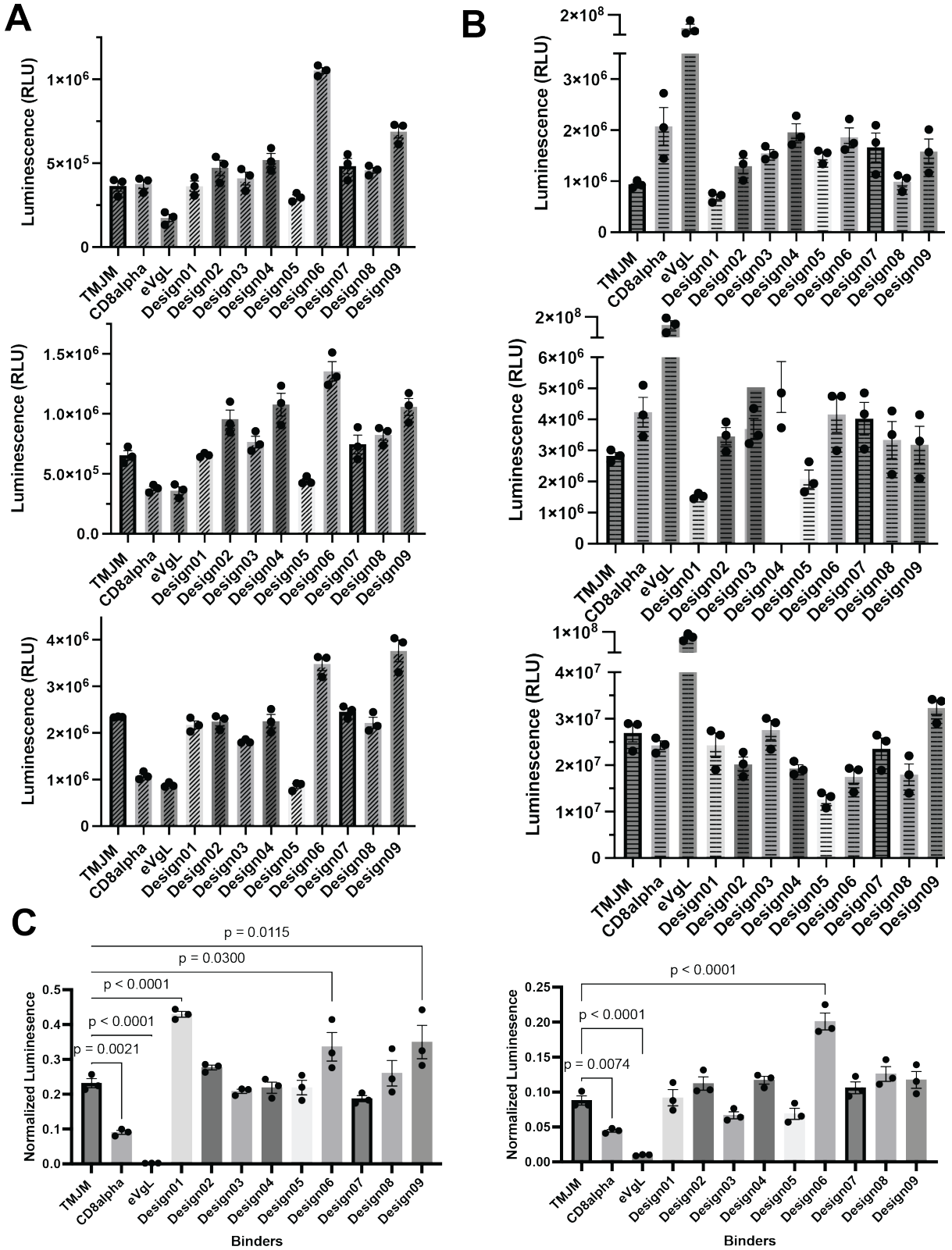


**Figure 7. Nanobit assay to quantify PPIs between *de novo* designs and TLR4 TMJM in cells. A)** NanoBit luminescence to self-complementation from protein-protein interactions between binder and target constructs where *de novo* designs were evaluated for their interaction capacity against TLR4 TMJM target (n=3 biological replicates). **B)** HiBit-based luminescence measurements used to quantify the amount of binder in in cell membranes during nanobit assay for evaluating design interaction capacity with TMJM (n=3 biological replicates). **C)** Normalized luminesce in biological replicates for the 9 *de novo* designed binders and the TMJM target.

Design 1 was derived from an initial backbone geometry predicted by TMHop. Its interface features 12 tightly packed **knobs-into-holes** interactions and a single core polar residue, threonine, which forms a hydrogen bond with its own backbone atoms in the preceding helical turn. Consequently, Design 1 primarily relies on van der Waals interactions from apolar residues for stability (Figure 8A). In contrast, Design 6 was built using an AlphaFold2-multimer-predicted backbone geometry (Figure 8B). The Design 6 model suggests that interface stabilization is achieved through a combination of hydrogen bonding and apolar packing: a predicted interchain hydrogen bond between TLR4 TM Ser640 and Design 6 Thr13, along with eight **knobs-into-holes** interactions distributed along the interface (Figure 8C). Despite Design 1 sharing Thr13 with Design 6, Design 1 does not appear to form the interchain hydrogen bond with TLR4 Ser640 and instead uses the methyl side chain of threonine for packing.

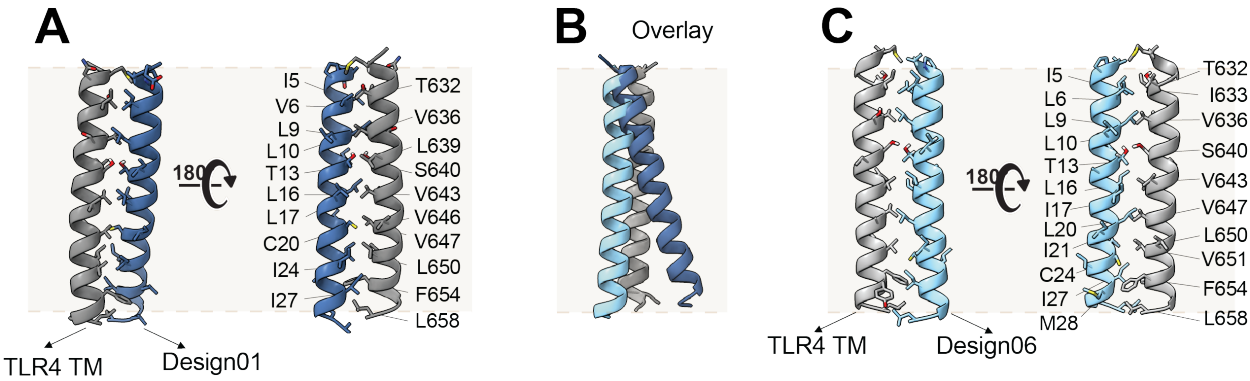


**Figure 8 Design models of TLR4 TMJM targetting peptides**
**A)** Design model of anti-TLR4 Design 1 and TLR4 TM domain, with interfacial side chains shown highlighting a side chain packing of apolar residues is driving feature establishing helix interface packing. **B)** Design 1 and Design 6 target were designed using different input backbone geometries to target distinct surfaces on the native TM helix. **C)** Design model of anti-TLR4 Design6 and TLR4 TM domain, with interfacial side chains shown highlighting an interchain hydrogen bond and optimized knobs into hole interactions with apolar residues.

To establish the sequence specificity of these lead anti-TLR4 TM proteins, we generated modified constructs with scrambled the primary sequences for the TM span of designs assayed interactions by Nanobit (Figure 10A). The scrambled Designs 1 and 6 exhibit consistently lower luminescence signal upon co-expression with TL4-TMJM, relative to the non-scrambled parent TM proteins (2.5±0.5 fold-change with $p = 0.002$ and 1.8±0.4 fold-change with $p=0.045$), exhibiting PPI signal similar to that of the high-expressing non-specific control protein CD8a (Figure 9A, Figure 10B). These results support that these computationally designed proteins targeting TLR4 is sequence specific, ruling out that is co-localization

due simply due to their TM length, amino acid composition i.e., being inherently greasy, or overcrowding in restricted bilayer spaces i.e., trafficking to similar membrane microdomains. Sequence-specific interaction with TLR4 TM domain through a computationally designed *de novo* protein demonstrates how molecular recognition is encodable in the bilayer without canonical interfaces and that TRL4 TM domains present tunable targeting surfaces.

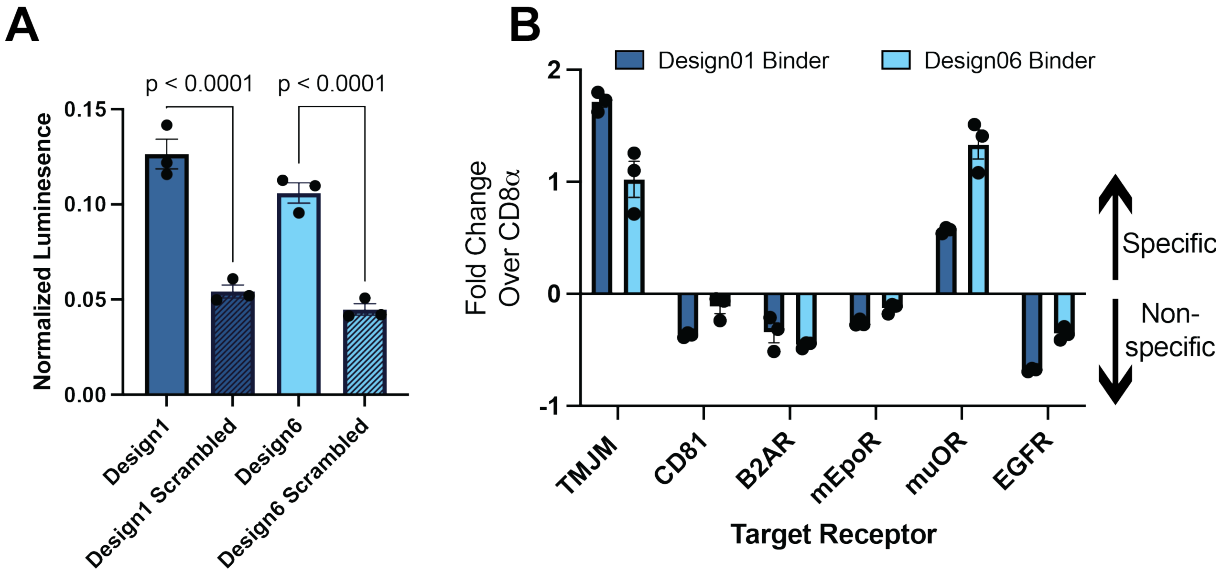


**Figure 9. Sequence and target specificity of lead anti-TLR4 TM *de novo* designs.**
A) The scrambled version of sequences for Design 1 and 6 had significantly lower normalized luminescence compared to corresponding original design binder in NanoBit, suggesting specific protein-protein interaction is encoded in the primary sequence of each lead design. **B)** The designs were assays with NanoBit to determine specificity against a panel of endogenous single and multi-pass membrane protein receptors. Values are reported as fold-change over non-specific control CD8alpha, where a value >1 indicates specific interaction and <1 indicates non-specific interactions with the target receptors.

We also evaluated the off-target interaction potential for Design 1 and Design 6 to determine if the designed targeting molecules would form complexes with the TLR4 target receptor more readily than alternate membrane proteins in the membrane. We measured the interaction potential for Designs 1, 6, and TMJM for a panel of endogenous single or multi-pass transmembrane immune receptors with a similar nanobit experiment. For all receptors in our panel except for muOpiod receptor, the Designs displayed lower or insignificantly more normalized luminescence than the non-specific CD8alpha binder control (Figure 9B, 4.10C). The observed off-target interactions with muOpiod receptor may be a result of Designs

trafficking to the same membrane sub-compartments as this target protein. Nonetheless, we preliminarily established our *de novo* designs are a unique molecular tool with TLR4 targeting capacity and minimal off-target interactions against target other proteins that reside in the lipid bilayer.

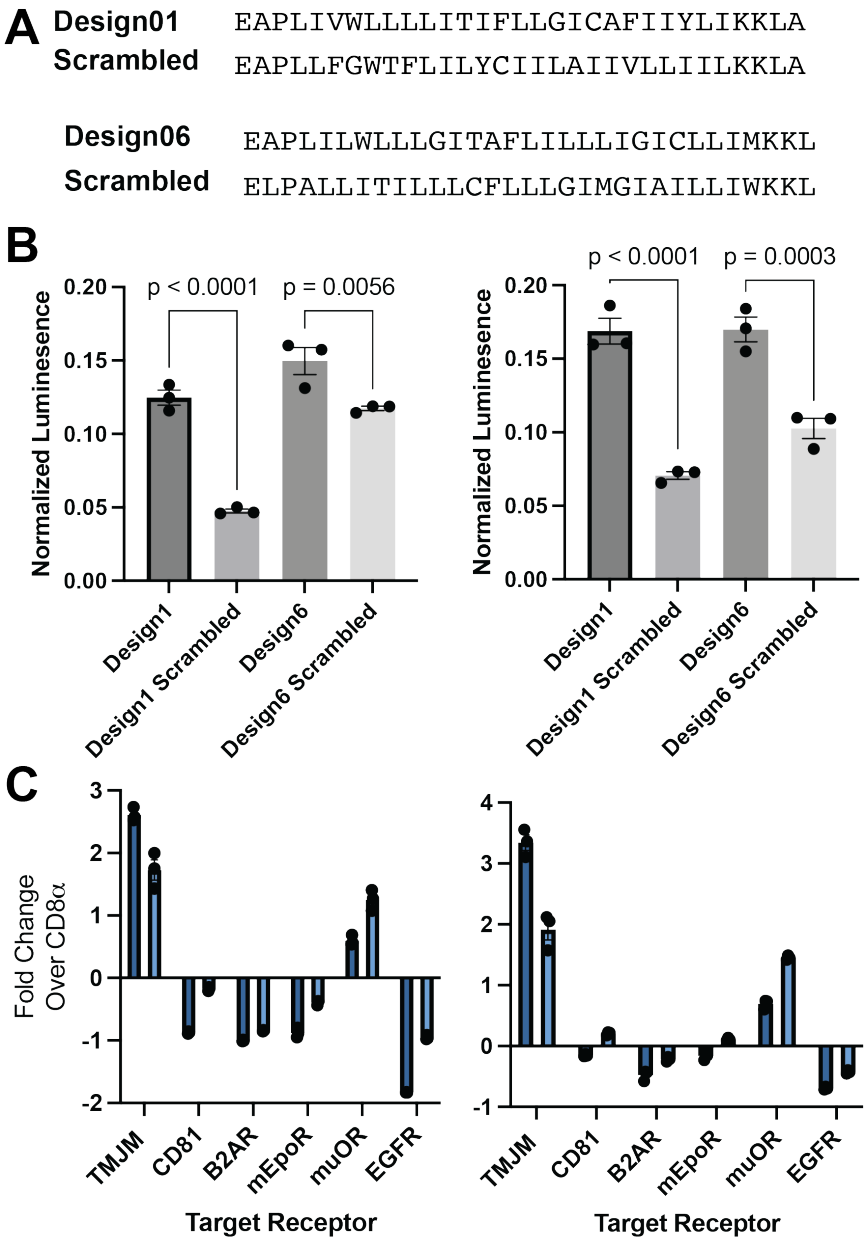


**Figure 10. Lead designs interact with TMJM in a sequence and target specific manner.**
**A)** Original and scrambled sequences used to test sequence specificity of the protein-protein interaction in cells have less than 80% sequence similarity. **B)** Biological replicates (n=3) of NanoBit assay with TMJM target and lead Designs 1 and 6 compared to their scrambled sequence versions reveals a sequence-specific interaction. **C)** Biological replicates (n=3) of NanoBit against a panel of endogenous single and multi-pass membrane protein receptors. Values are reported as fold-change over non-specific control CD8alpha, where a value >1 indicates specific interaction and <1 indicates non-specific interactions with the target receptors.

**Design6 inhibits NF-κB signaling in sequence- and dose-dependent manner.**

The successful development of native and synthetic molecular targeting tools against the TLR4 TMJM domain prompted us to evaluate their ability to interact with full-length receptor target and in turn manipulate the cross-membrane signaling mechanism of TLR4. Ultimately, we aimed assess whether the TLR4's TM native interactions and inter-domain geometry is crucial for its long-range conformational coupling for cross-membrane signal activation.

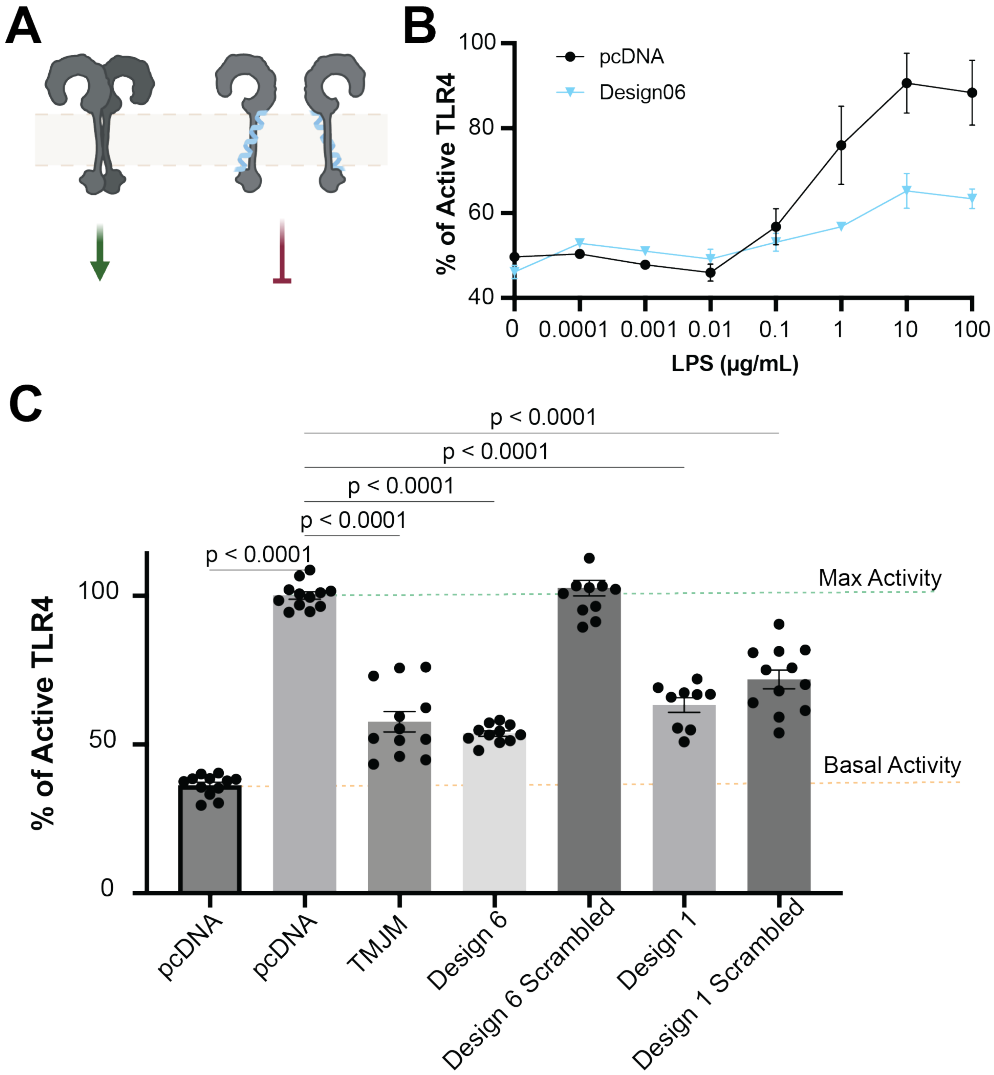


**Figure 11. Anti-TLR4 Design 6 specifically inhibits LPS induced NF-κB signaling.**
**A)** Proposed model of inhibition where native TM interactions are required to transmit signal from outside to inside via an active receptor complex. A anti-TLR4 TM targeting peptide will disrupt active receptor complex signaling via steric disruption of the crucial TM-TM interactions within the lipid bilayer. **B)** LPS dose curve for TLR4 co-transfected with Design 6 shows lower overall activity compared to TLR4 co-transfected with an empty vehicle, consistent with a non-competitive inhibitor. **C)** Plasmid DNA of an empty vehicle, lead designs, or scrambled versions of lead designs was delivered to an NFkB reporter cells co-transfected with TLR4. When treated with 10 ug/mL LPS and analyzed for activation, Design 6 inhibited specifically compared to its scrambled version while Design 1 and Design 1 scrambled both inhibited moderate levels suggesting an off-target effect (n=3).

We reasoned that the native TMJM protein could elicit competing protein-protein interaction in the membrane would disrupt formation of the active receptor dimeric complex and inhibit NF-κB signaling downstream of LPS-stimulated TLR4 via lowering overall efficacy or shifting EC50 (Figure 11A). To test this hypothesis, we used a colorimetric assay in a reporter cell line expressing NF-κB-inducible secreted embryonic alkaline phosphatase, along with co-receptors MD2 and CD14.

In this system, TLR4-GFP was activated 63.7±3.7% (n=3) above basal levels with 10 μg/mL LPS when co-transfected with pcDNA control plasmid (Figure 11C). The LPS induced activity of TLR4-eGFP with plasmid DNA delivery of the isolated TMJM fused to largeBit was only 22.5±12.8% (n=3) above basal levels, meaning a 41.2±11.7% reduction in max signaling capacity (Figure 11C). Since TMJM-mediated inhibition correlated with a measurable protein-protein interaction, this result underscores the role of native TLR4 cross-membrane interactions in receptor activation and establishes TLR TM fragments as dominant negative inhibitor well suited to probing membrane-spanning mechanisms.

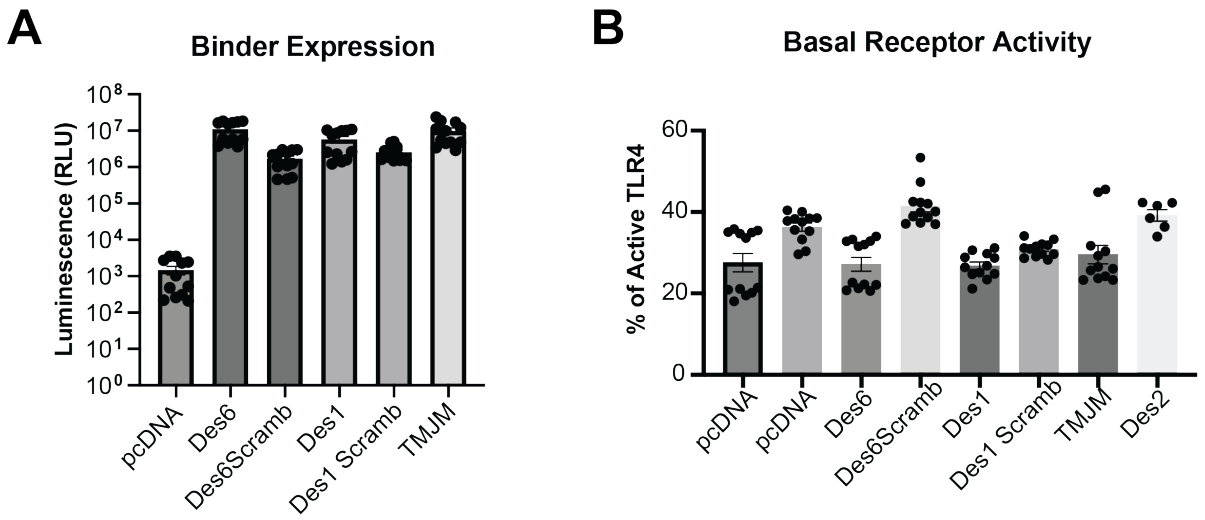


**Figure 12. Inhibitory function of TM proteins interacting with TLR4.**
**A)** Controls or lead designs that were co-transfected in 293T cells displayed similar binder expression levels as measured by HiBit luminescence in biological replicates (n=3). **B)** The basal NFkB response for TLR4 co-transfections with controls of Designs was not significantly different depending on the challenge protein introduced in biological replicates (n=3).

We then evaluated the ability for synthetic designs to hinder TLR4 activation through interaction with full-length receptors in mammalian cells. We measured the effect of Design 6 fused to largeBit on TLR4-eGFP activity and observed a minimal 18.2±6.0% (n=3) increase in activity above basal with LPS agonism (46.7±3.0% reduction from max signaling capacity, Figure 11C). In contrast, its scrambled variant (Design 6 Scrambled) slightly increased TLR4-eGFP max signaling capacity by 3.54±9.1% (n=3), confirming that Design 6's inhibitory effect is sequence-specific and dependent on targeted protein-protein interactions with the TMJM region of TLR4 (Figure 11C). Importantly, there was not a large variability in TM targeting protein expression levels and basal activity was not significantly different across each challenged condition (Figure 12). To investigate the mechanism of inhibition, we then measured an LPS dose-dependent activation curve for unchallenged or Design 6 challenged TLR4 activity. Design 6 reduced the maximal response but did not shift the $EC_{50}$ value of LPS (Figure 11B), supporting a model where native and synthetic transmembrane protein sterically blocks the active receptor conformation to prevent downstream signaling.

We further demonstrated Design 6 also presents a dose-dependent inhibition response. HiBit luminescence served a metric to quantify the amount of Design 6 fused to largeBit in cells and affirms that increasing DNA amounts boosts total protein amount of Design 6 in each condition (Figure 13B). Increased concentrations of Design 6 in cells resulted in increased inhibition activity also with a sigmoid like curve, while total TLR4 levels remained unaffected (n=1, Figure 13A,C,D). These findings establish evidence for sequence dependent and preliminary evidence for dose-dependent bioactivity of this peptide. These data also support a mechanistic model where molecular targeting is synthetically encoded to intervene with native protein-protein interactions in the bilayer and disrupt receptor activity.

Interestingly, delivering Design 1 as plasmid DNA with largeBit fused displayed moderate inhibition, reducing LPS-induced TLR4-NF-κB signaling efficacy by 35.1±7.4% (n=3), but lacked sequence-specific bioactivity. Design 1-Scrambled also reduced TLR4 signaling capacity by 26.6±10.9% (n=3), despite that evidence that scrambled proteins did not specifically interact with the TLR4 TM in our

protein-protein interaction assay (Figure 11C). This result put into question that Design 1 and Design 1 Scrambled may operate through an alternative inhibition mechanism, rather than direct modulation of TLR4 structure and activity.

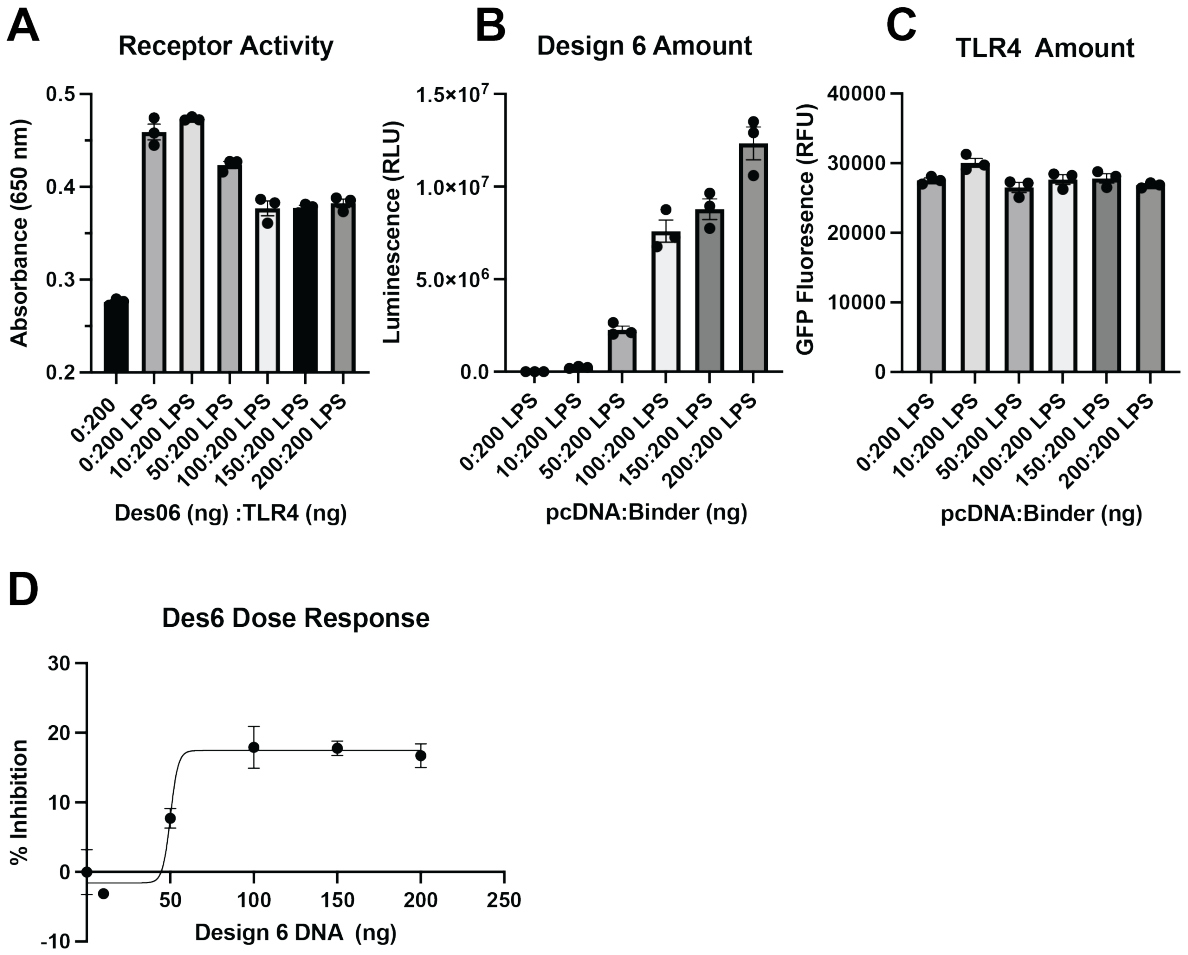


**Figure 13. Design 6 induces dose-dependent inhibition for LPS activation in TLR4.**
**A)** NFkB response to 10 ug/mL LPS decreases with increasing amounts of Design 6 co-transfected in HEK-Blue cells with TLR4. **B)** The amount of Design 6, quantified by HiBit luminescence increases as the DNA ratio increases relative to pcDNA in TLR4 co-transfections in 293T cells. **C)** The difference in receptor expression was monitored by TLR4-GFP fluorescence and deemed not significant (ANOVA, p=>0.5) eliminating degradation of TLR4 is the primary mechanism of inhibition for lead designs. **D)** Relative to TLR4 with no Design 6 challenge, the percent of % inhibition increases as amount of Design 6 challenge protein increases, following a sigmoidal trend akin to dose-dependent responses.

## Biophysical Characterization of TMJM Complexed with Lead Designs

To measure the formation of a biochemically stable complex with TLR4 in the mammalian cell environment, we also performed co-immunoprecipitation. Cell membranes co-expressing TMJM target and

Design 6, TMJM, or eVgL bait were solubilized in DDM:CHS. Flag-tagged bait proteins were pulled down and an HA specific band corresponding to TMJM target protein was observed in each Design 6 and TMJM co-transfected conditions. The relative band intensity shows Design 6 bait pulls down more TMJM protein than the TMJM bait, confirming the observed in-cell protein-protein interactions are sustained in vitro (Figure 15C).

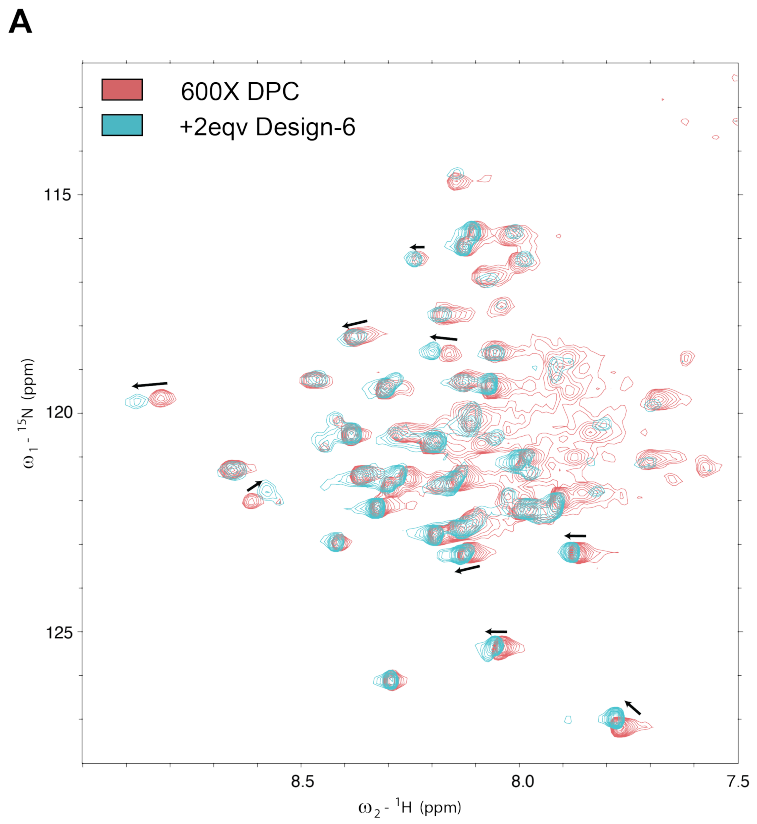


**Figure 14. Solution NMR of TLR4-TMJM or the stable complex between TLR4-TMJM with Design 6 in DPC micelles**
A) The $^1$H-$^{15}$N HSQC spectra of 0.2 mM $^{15}$N His-TMJM at 40 °C, pH 6.0, and 800 MHz at 600X (red) or 180X 2H-DPC (Light Blue-green) with Design-6. Reference spectra (no Design-6, red) represents the monomeric state of $^{15}$N His-TMJM (molar ratio of DPC to $^{15}$N His-TMJM is 600X). Addition of 2 molar equivalents (eqv) of Anti-TLR4 Design-6 to 0.2mM $^{15}$N His-TMJM in 36mM DPC (Light Blue-green, 60x ratio detergent to total peptide, 180x DPC to TMJM; 1% mol fraction Design-6) show significant chemical shift perturbations that are distinct from those associated with TLR4-TMJM homo-oligomerization. Arrows label the significant peak shifts observed and most of the chemical shift perturbations are in opposite directions as observed in TMJM homo-oligomerization events.

To investigate the direct interaction with the TM segment of TLR4 *in vitro*, we measured the solution NMR spectra of an U-$^{15}$N TLR4-TMJM protein fragment with or without the presence of Design 6 as a minimal unlabeled TM peptide in $^2$H-DPC micelles (Figure 14, Table 41 of those peptide sequences).

We first explored the detergent-dependent self-interaction of this TLR4 TMJM fragment alone, varying DPC molar ratio to protein at 600x, 180x, and 60x (Fig 14, 15). The TLR4 fragment exhibits chemical shift perturbations and broadening in its $^{1}H$-$^{15}N$ HSQC spectra for between 600x and 180x, indicative of likely homo-dimerization as seen previously[28], with apparent fast exchange. At 60x, (~1 protein per micelle on average, near-crowding), TLR4 TMJM peaks further broaden, and some additional shifts occur but often in directions distinct from those perturbations between 600x and 180x, indicating mixtures of additional higher-order homo-assemblies, also seen previously[28]. When TLR4 TMJM at 180x is reconstituted with 2 equivalents of Design-6, the spectra are broadly perturbed in fast-exchange relative to TLR4-TMJM's spectra alone at 180x (likely homo-dimeric conditions) or at 600x (likely monomeric conditions) (Fig 14.4b). Design-6 induces a unique chemical environment for TLR-TMJM indicative of a direct complex stable to the 45° C and zwitterionic detergent micelle conditions. Given Design-6 does not induce further resonance broadening than TLR4-TMJM alone at 180x, and rather sharpens resonances, we believe the distinct perturbations are indicative of a unique hetero-dimeric complex rather than Design-6 binding the homodimer. Likewise, based on distinct chemical shift perturbation directions, formation of the Design-6-TMJM complex appears to be competitive with the homo-dimerization, which might indicate that Design-6 binds the TLR4 at a helix surface which is overlapping and mutually exclusive with its homo-dimerization interface. Thus, we found that *de novo* designed TM proteins successfully screened out of a cell-based assay for PPI to TLR4 inhibited LPS-induced NF-κB signaling and indeed form a competitive transmembrane-direct complex in solution stable to a harsh detergent condition, which aligns with the intended mechanism of immune signaling antagonism by a designed membrane adaptor complex.

Collectively, these findings demonstrate that both native and synthetic transmembrane-targeting peptides can modulate TLR4 activation by disrupting its TM-mediated cross-membrane protein interactions and signaling. By leveraging *de novo* design to encode sequence-specific interactions within the bilayer, we confirmed designed proteins in-cell and in vitro complex formation with the TLR4 TM domain. This expands protein design capability and presents a versatile blueprint for engineering targeted modulators

that intervene in receptor activation by selectively competing with native TM-driven dimerization.

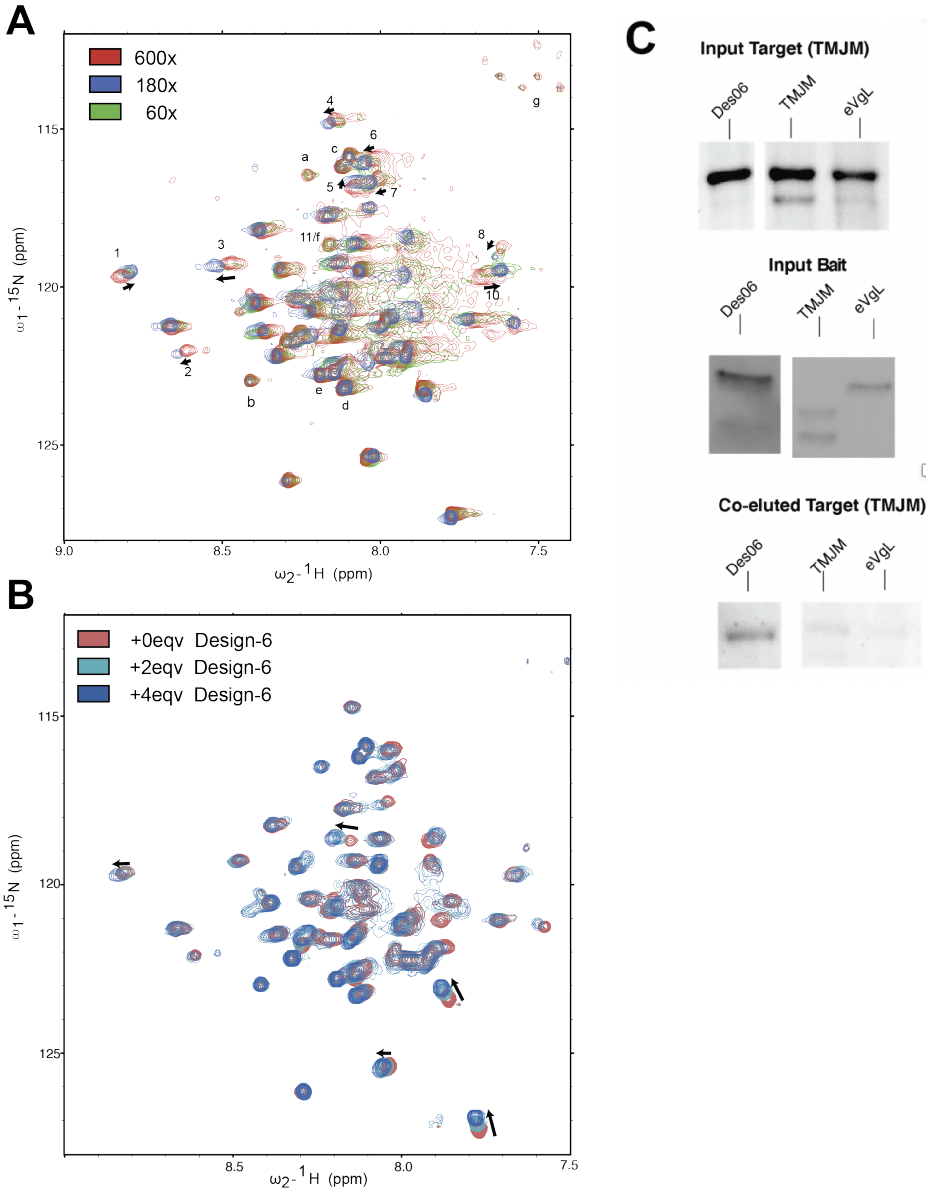


**Figure 15. In vitro biophysical analysis and in-cell biochemical of Design 6-TMJM interaction.**
**A)** The $^{1}$H-$^{15}$N HSQC spectra of 0.2 mM $^{15}$N His-TMJM at 40 °C, pH 6.0, and 800 MHz at 60, 180, and 600 molar equivalents of detergent (12mM, green, 36mM, blue, and 120mM, red). The more concentrated sample (180x, blue) shows a set of peak shift compared to the diluted sample (600X, red), which likely representing the peak shift caused by change from monomeric state (600X DPC) to homodimeric state (180X). Peak shift directions are marked by black arrows on the spectra. The most concentrated sample (60X, green) shows overall weaker signal but similar peak shift trend as 180X sample.**B)** The $^{1}$H-$^{15}$N HSQC spectra of 0.2 mM $^{15}$N His-TMJM in 60mM n-Dodecyl-phosphocholine (DPC) at 40 °C, pH 6.0, and 800 MHz when titrated with Anti-TLR4 Design-6 at 0, 2, and 4 molar equivalents of binder (0mM, red, 0.4mM, Light-Blue-green, and 0.8mM, Blue). As more Anti-TLR4 Design6 binder were titrated, the spectra shows a continuous shift of a set of peaks (marked by arrows) suggesting a fast exchange interaction between TLR4 TMJM and Anti-TLR4 Design-6. **C)** Co-immunoprecipitation experiments with Flag-tagged TMJM bait pull down more HA-tagged Design 6 target compared to HA-tagged TMJM target or HA-tagged eVgL target when expressed in HEK293T cells and solubilized in DDM:CHS.

## Discussion

In this study, we established that the membrane-spanning region of TLR4 is a viable and physiologically relevant molecular surface for modulating receptor function. This fundamental biochemical principle, established for other single pass transmembrane receptors but unrealized for TLR4, enabled us to develop molecular technologies to probe mechanistic hypotheses regarding receptor structure and function. We confirmed that minimal membrane-spanning receptor components (TM and TMJM) form homo-oligomeric protein-protein interactions in cells and demonstrated that the TMJM peptide can disrupt native receptor activation. These findings suggest a new governing principle for TLR4 signaling: receptor activation is modulated by native membrane-spanning interactions to some degree, with the TMJM domain acting as a dominant-negative regulator.

We explored synthetic molecules as tools for studying structure-function relationships. Prior computational design methods were not well suited for engineering TLR4 TM adaptor proteins, as predicted interactions between TLR4 TM domains failed to converge across structural modeling approaches, including co-evolutionary analysis, NMR-derived chemical shifts, AlphaFold2 predictions, and TMHop modeling[25,28–32]. Additionally, the TLR family lacks a distinct dimerization motif, complicating the grafting of initial backbone interaction geometries.

To address these challenges, we executed a fully ***de novo*** design pipeline using Rosetta-design to target receptor TM spans without relying on known homo-dimerization structures as templates or sequence motifs known interactions, as done previously[2,4–6]. Our work expands upon a similar approach used for designed point mutants to improve of mimic TM peptides[2]. Beyond energetic calculations, we prioritized inter-chain hydrogen bonds and apolar side-chain packing to construct stable, realistic peptides in silico. All selected designs expressed in mammalian cells, with most localizing to the plasma membrane in the intended Type I orientation. Several formed interactions with TMJM at levels exceeding those expected from overcrowding or non-specific binding. While not all interactions were sequence-specific, we

successfully generated two molecular targeting tools with potential for future protein engineering applications.

Our anti-TLR4 TM designs demonstrate that TM-targeting molecules can be engineered without requiring sequence or structural templates. This multi-pronged computational strategy integrates structural modeling, sequence design, and customized TM interface evaluation metrics to establish a broadly applicable framework for membrane protein targeting. By eliminating dependence on predefined interaction motifs, we expanded the range of immune receptors that can be targeted and increased design flexibility for TM adaptors to tuning receptors function with diverse geometries and interaction interfaces.

Interestingly, current deep learning-based structure prediction methods do not accurately capture our design models, possibly due to the distinct physiochemical environment of a lipid bilayer. Also, the evolutionary constraints for membrane protein folding compared to soluble proteins present inherent challenges associated with modeling and designing membrane protein interactions with machine learning algorithms. The synthetic nature of our designs may evade evolutionary trends that the prediction methods are typically well poised to model. Alternatively, the membrane-specific folding principles underlying our designed interactions may not be pronounced by current deep learning models, due to the distinct nature of membrane protein folding and the minimal contribution of membrane proteins to the total proteome compared to soluble proteins used for training. It is possible that training deep learning-based structure prediction models on a membrane-centric dataset could improve the accuracy of membrane protein fold predictions. We also cannot exclude the possibility that our designs might not be forming the intended interfaces in vivo.

Nonetheless, our sequence-specific TLR4 TM-targeting protein designs had functional consequences for TLR4 signaling and identified a new way to modulate TLR4 activity. By using synthetic peptide sequences to elicit bioactivity, we can likely overcome specificity issues associated with using the dominant negative TMJM as an antagonistic molecule. Design 6 was identified as an effective, largely

target-specific, and dose-dependent inhibitor. We can conclude that its mechanism of action is via structural perturbation, as no decrease in TLR4 expression was observed with increasing Design 6 concentration, and overall signaling efficacy was decreased while EC50 values remained unchanged.

While our study combines in silico, in-cell, and in vitro assays, further studies are needed to fully assess the therapeutic potential of Design 6, particularly in physiologically relevant models. Its activity must be validated in physiologically relevant cell lines, and considerations for potency, metabolism, developability, and delivery mechanisms are essential. Formulating as synthetic peptides in liposomal vesicles or genes via mRNA delivery can introduce these functional *de novo* TM adaptor sequences safely and effectively to cell membranes and has potential to mitigate the low solution solubility of the hydrophobic TM peptides. Those improvements could make these technologies viable to explore for developing translationally relevant molecules. Nevertheless, the precise design of an anti-inflammatory molecule targeting the TLR4 TM domain represents an exciting step toward developing targeted therapies for conditions such as sepsis, colitis, cancer, and autoimmune disorders, bacterial or viral infections, and allergies.

In contrast, the interaction between TMJM and Design 1 was sequence-specific, but did not result in bioactivity. This may be due to the peptide targeting a non-consequential surface of the TLR4 TM domain, a limitation expected when our design sampled multiple protein interaction surfaces without knowing which might be competitive with receptor dimerization and signaling. Our successful targeting designs present opportunities for expanding protein design approaches, including the incorporation of E3 ligases for targeted protein degradation or the use of scaffolds to enhance the stability of the membrane-spanning region for structural characterization[33–35].

Additionally, the TM domains of all TLRs are largely non-homologous. This aspect motivates future efforts to conduct a family-wide TM adaptor design campaign, where our design methods can be implemented to develop of a streamlined toolbox of TM-targeting peptides tailored to each receptor,

enabling unique probing of receptor function and structural mechanisms[36]. Ultimately, our breakthrough in protein design not only yields new insights into TLR4 mechanisms but also sets a powerful precedent for targeting transmembrane adaptor proteins, paving way towards a new era of computationally engineered therapies for a wide array of diseases and providing a robust framework for manipulating membrane protein interactions with specificity and control.

**Competing Interests.**

A patent application (US Patent Application No. 63/799,795) covering the TM-targeting peptides and strategies described in this work has been filed by the authors (CAM, ABW, MM) .

**Acknowledgements.**

We extend deep gratitude to Kathryn Spencer at the Microscopy Core Facility for their technical support, JC Ducom at the High-Performance Computing (HPC) cluster for their assistance, and Gerard Kroon for technical assistance on NMR data collection and processing at Scripps Research Institute. We are also immensely grateful to Weiyi Tang, Sebastian Jojoa-Cruz, Monica Fernández Quintero, Stefano Forli, and Keren Lasker for insightful discussions throughout the course of this work. We also extend thanks to Ian Wilson for his valuable feedback on the manuscript draft. C.A.M was supported by the John & Susan Diekman Endowed Fellowship and ARCS Foundation – San Diego Chapter.

**References**

(1) Bloch, E.; Sikorski, E. L.; Pontoriero, D.; Day, E. K.; Berger, B. W.; Lazzara, M. J.; Thévenin, D. Disrupting the Transmembrane Domain–Mediated Oligomerization of Protein Tyrosine Phosphatase Receptor J Inhibits EGFR-Driven Cancer Cell Phenotypes. *J Biol Chem* **2019**, *294* (49), 18796–18806. https://doi.org/10.1074/jbc.RA119.010229.

(2) Duart, G.; Elazar, A.; Weinstein, J. Y.; Gadea-Salom, L.; Ortiz-Mateu, J.; Fleishman, S. J.; Mingarro, I.; Martinez-Gil, L. Computational Design of BclxL Inhibitors That Target Transmembrane Domain Interactions. *Proc Natl Acad Sci U S* . **2023**, *120* (11), e2219648120. https://doi.org/10.1073/pnas.2219648120.

(3) Mravic, M.; Hu, H.; Lu, Z.; Bennett, J. S.; Sanders, C. R.; Orr, A. W.; DeGrado, W. F. De Novo Designed Transmembrane Peptides Activating the A5β1 Integrin. *Prot Eng Des Sel* **2018**, *31* (5), 181–190. https://doi.org/10.1093/protein/gzy014.

(4) Mravic, M.; He, L.; Kratochvil, H. T.; Hu, H.; Nick, S. E.; Bai, W.; Edwards, A.; Jo, H.; Wu, Y.; DiMaio, D.; DeGrado, W. F. De Novo-Designed Transmembrane Proteins Bind and Regulate a Cytokine Receptor. *Nat Chem Biol* **2024**, *20* (6), 751–760. https://doi.org/10.1038/s41589-024-01562-z.

(5) Yin, H.; Slusky, J. S.; Berger, B. W.; Walters, R. S.; Vilaire, G.; Litvinov, R. I.; Lear, J. D.; Caputo, G. A.; Bennett, J. S.; DeGrado, W. F. Computational Design of Peptides That Target Transmembrane Helices. *Science* **2007**, *315* (5820), 1817–1822. https://doi.org/10.1126/science.1136782.
(6) Caputo, G. A.; Litvinov, R. I.; Li, W.; Bennett, J. S.; DeGrado, W. F.; Yin, H. Computationally Designed Peptide Inhibitors of Protein−Protein Interactions in Membranes. *Biochemistry* **2008**, *47* (33), 8600–8606. https://doi.org/10.1021/bi800687h.
(7) Fink, A.; Reuven, E. M.; Arnusch, C. J.; Shmuel-Galia, L.; Antonovsky, N.; Shai, Y. Assembly of the TLR2/6 Transmembrane Domains Is Essential for Activation and Is a Target for Prevention of Sepsis. *J Immunol* **2013**, *190* (12), 6410–6422. https://doi.org/10.4049/jimmunol.1202033.
(8) Gross-Vered, M.; Shmuel-Galia, L.; Zarmi, B.; Humphries, F.; Thaiss, C.; Salame, T.-M.; David, E.; Chappell-Maor, L.; Fitzgerald, K. A.; Shai, Y.; Jung, S. TLR2 Dimerization Blockade Allows Generation of Homeostatic Intestinal Macrophages under Acute Colitis Challenge. *The J Immunol* **2020**, *204* (3), 707–717. https://doi.org/10.4049/jimmunol.1900470.
(9) Godfroy, J. I.; Roostan, M.; Moroz, Y. S.; Korendovych, I. V.; Yin, H. Isolated Toll-like Receptor Transmembrane Domains Are Capable of Oligomerization. *PLoS ONE* **2012**, *7* (11), e48875. https://doi.org/10.1371/journal.pone.0048875.
(10) Panter, G.; Jerala, R. The Ectodomain of the Toll-like Receptor 4 Prevents Constitutive Receptor Activation. *J Biol Chem* **2011**, *286* (26), 23334–23344. https://doi.org/10.1074/jbc.M110.205419.
(11) Treeby, M.; Vašl, J.; Ota, P.; Friedrich, J.; Jerala, R. Different Functional Role of Domain Boundaries of Toll-like Receptor 4. *Biochem Biophys Res Commun* **2009**, *381* (1), 65–69. https://doi.org/10.1016/j.bbrc.2009.02.017.
(12) Kuzmich, N.; Sivak, K.; Chubarev, V.; Porozov, Y.; Savateeva-Lyubimova, T.; Peri, F. TLR4 Signaling Pathway Modulators as Potential Therapeutics in Inflammation and Sepsis. *Vaccines* **2017**, *5* (4), 34. https://doi.org/10.3390/vaccines5040034.
(13) Anwar, M. A.; Shah, M.; Kim, J.; Choi, S. Recent Clinical Trends in Toll-like Receptor Targeting Therapeutics. *Med Res Rev* **2019**, *39* (3), 1053–1090. https://doi.org/10.1002/med.21553.
(14) Alves, D. S.; Westerfield, J. M.; Shi, X.; Nguyen, V. P.; Stefanski, K. M.; Booth, K. R.; Kim, S.; Morrell-Falvey, J.; Wang, B.-C.; Abel, S. M.; Smith, A. W.; Barrera, F. N. A Novel pH-Dependent Membrane Peptide That Binds to EphA2 and Inhibits Cell Migration. *eLife* **2018**, *7*, e36645. https://doi.org/10.7554/eLife.36645.
(15) Westerfield, J. M.; Barrera, F. N. Membrane Receptor Activation Mechanisms and Transmembrane Peptide Tools to Elucidate Them. *J Biol Chem* **2020**, *295* (7), 1792–1814. https://doi.org/10.1074/jbc.REV119.009457.
(16) Partridge, A. W.; Melnyk, R. A.; Yang, D.; Bowie, J. U.; Deber, C. M. A Transmembrane Segment Mimic Derived from Escherichia Coli Diacylglycerol Kinase Inhibits Protein Activity. *J Biol Chem* **2003**, *278* (24), 22056–22060. https://doi.org/10.1074/jbc.M210685200.
(17) Yin, H.; Litvinov, R. I.; Vilaire, G.; Zhu, H.; Li, W.; Caputo, G. A.; Moore, D. T.; Lear, J. D.; Weisel, J. W.; DeGrado, W. F.; Bennett, J. S. Activation of Platelet αIIbβ3 by an Exogenous Peptide Corresponding to the Transmembrane Domain of αIIb. *J Biol Chem* **2006**, *281* (48), 36732–36741. https://doi.org/10.1074/jbc.M605877200.
(18) He, L.; Shobnam, N.; Hristova, K. Specific Inhibition of a Pathogenic Receptor Tyrosine Kinase by Its Transmembrane Domain. *Biochim Biophys Acta (BBA) - Biomembranes* **2011**, *1808* (1), 253–259. https://doi.org/10.1016/j.bbamem.2010.08.007.
(19) Korendovych, I. V.; DeGrado, W. F. *De Novo* Protein Design, a Retrospective. *Quart. Rev. Biophys.* **2020**, *53*, e3. https://doi.org/10.1017/S0033583519000131.
(20) Kortemme, T. De Novo Protein Design—From New Structures to Programmable Functions. *Cell* **2024**, *187* (3), 526–544. https://doi.org/10.1016/j.cell.2023.12.028.
(21) Vorobieva, A. A. Principles and Methods in Computational Membrane Protein Design. *J Mol Biol* **2021**, *433* (20), 167154. https://doi.org/10.1016/j.jmb.2021.167154.

(22) Moore, D. T.; Berger, B. W.; DeGrado, W. F. Protein-Protein Interactions in the Membrane: Sequence, Structural, and Biological Motifs. *Structure* **2008**, *16* (7), 991–1001. https://doi.org/10.1016/j.str.2008.05.007.
(23) Russ, W. P.; Engelman, D. M. The GxxxG Motif: A Framework for Transmembrane Helix-Helix Association. *J Mol Biol* **2000**, *296* (3), 911–919. https://doi.org/10.1006/jmbi.1999.3489.
(24) Alford, R. F.; Fleming, P. J.; Fleming, K. G.; Gray, J. J. Protein Structure Prediction and Design in a Biologically Realistic Implicit Membrane. *Biophys J* **2020**, *118* (8), 2042–2055. https://doi.org/10.1016/j.bpj.2020.03.006.
(25) Weinstein, J. Y.; Elazar, A.; Fleishman, S. J. A Lipophilicity-Based Energy Function for Membrane-Protein Modelling and Design. *PLoS Comput Biol* **2019**, *15* (8), e1007318. https://doi.org/10.1371/journal.pcbi.1007318.
(26) Reyes-Alcaraz, A.; Lucero Garcia-Rojas, E. Y.; Merlinsky, E. A.; Seong, J. Y.; Bond, R. A.; McConnell, B. K. A NanoBiT Assay to Monitor Membrane Proteins Trafficking for Drug Discovery and Drug Development. *Commun Biol* **2022**, *5* (1), 212. https://doi.org/10.1038/s42003-022-03163-9.
(27) Abramson, J.; Adler, J.; Dunger, J.; Evans, R.; Green, T.; Pritzel, A.; Ronneberger, O.; Willmore, L.; Ballard, A. J.; Bambrick, J.; Bodenstein, S. W.; Evans, D. A.; Hung, C.-C.; O'Neill, M.; Reiman, D.; Tunyasuvunakool, K.; Wu, Z.; Žemgulytė, A.; Arvaniti, E.; Beattie, C.; Bertolli, O.; Bridgland, A.; Cherepanov, A.; Congreve, M.; Cowen-Rivers, A. I.; Cowie, A.; Figurnov, M.; Fuchs, F. B.; Gladman, H.; Jain, R.; Khan, Y. A.; Low, C. M. R.; Perlin, K.; Potapenko, A.; Savy, P.; Singh, S.; Stecula, A.; Thillaisundaram, A.; Tong, C.; Yakneen, S.; Zhong, E. D.; Zielinski, M.; Žídek, A.; Bapst, V.; Kohli, P.; Jaderberg, M.; Hassabis, D.; Jumper, J. M. Accurate Structure Prediction of Biomolecular Interactions with AlphaFold 3. *Nature* **2024**, *630* (8016), 493–500. https://doi.org/10.1038/s41586-024-07487-w.
(28) Mineev, K. S.; Goncharuk, S. A.; Goncharuk, M. V.; Volynsky, P. E.; Novikova, E. V.; Aresinev, A. S. Spatial Structure of TLR4 Transmembrane Domain in Bicelles Provides the Insight into the Receptor Activation Mechanism. *Sci Rep* **2017**, *7* (1), 6864. https://doi.org/10.1038/s41598-017-07250-4.
(29) Hopf, T. A.; Colwell, L. J.; Sheridan, R.; Rost, B.; Sander, C.; Marks, D. S. Three-Dimensional Structures of Membrane Proteins from Genomic Sequencing. *Cell* **2012**, *149* (7), 1607–1621. https://doi.org/10.1016/j.cell.2012.04.012.
(30) Hopf, T. A.; Green, A. G.; Schubert, B.; Mersmann, S.; Schärfe, C. P. I.; Ingraham, J. B.; Toth-Petroczy, A.; Brock, K.; Riesselman, A. J.; Palmedo, P.; Kang, C.; Sheridan, R.; Draizen, E. J.; Dallago, C.; Sander, C.; Marks, D. S. The EVcouplings Python Framework for Coevolutionary Sequence Analysis. *Bioinformatics* **2019**, *35* (9), 1582–1584. https://doi.org/10.1093/bioinformatics/bty862.
(31) Marks, D. S.; Colwell, L. J.; Sheridan, R.; Hopf, T. A.; Pagnani, A.; Zecchina, R.; Sander, C. Protein 3D Structure Computed from Evolutionary Sequence Variation. *PLoS ONE* **2011**, *6* (12), e28766. https://doi.org/10.1371/journal.pone.0028766.
(32) Mirdita, M.; Schütze, K.; Moriwaki, Y.; Heo, L.; Ovchinnikov, S.; Steinegger, M. ColabFold: Making Protein Folding Accessible to All. *Nat Methods* **2022**, *19* (6), 679–682. https://doi.org/10.1038/s41592-022-01488-1.
(33) Siepe, D. H.; Picton, L. K.; Garcia, K. C. Receptor Elimination by E3 Ubiquitin Ligase Recruitment (REULR): A Targeted Protein Degradation Toolbox. *ACS Synth Biol* **2023**, *12* (4), 1081–1093. https://doi.org/10.1021/acssynbio.2c00587.
(34) Cui, J.; Zheng, Q.; Weng, Y.; Zhai, X.; Su, Z.; Du, Y.; Wei, X.; Yu, Y.; Qu, Q.; Pan, M. Structure-Guided Development of Chemically Tailored Peptide Binders of RNF43/ZNRF3 to Enable Versatile Design of Membrane Protein-Targeting PROTACs. *Angew Chem Int Ed* **2025**, e202501488. https://doi.org/10.1002/anie.202501488.
(35) Errasti-Murugarren, E.; Bartoccioni, P.; Palacín, M. Membrane Protein Stabilization Strategies for Structural and Functional Studies. *Membranes* **2021**, *11* (2), 155. https://doi.org/10.3390/membranes11020155.
(36) Hajishengallis, G.; Lambris, J. D. More than Complementing Tolls: Complement–Toll-like Receptor Synergy and Crosstalk in Innate Immunity and Inflammation. *Immunol Rev* **2016**, *274* (1), 233–244. https://doi.org/10.1111/imr.12467.

(37) Lee, W.; Tonelli, M.; Markley, J. L. NMRFAM-SPARKY: Enhanced Software for Biomolecular NMR Spectroscopy. *Bioinfor* **2015**, *31* (8), 1325–1327. https://doi.org/10.1093/bioinformatics/btu830.